Astronomical and Astrophysical Transactions (*AApTr*), 2021, Vol. 32, Issue 3, pp. 241–248,
ISSN 1055-6796, Photocopying permitted by license only, ©Cambridge Scientific Publishers

Radio observations of solar active regions at 7.36 and 37 GHz

Juha Kallunki[1,*], Merja Tornikoski[1], Dmitrijs Bezrukovs[2]

[1] *Metsähovi Radio Observatory, Aalto University, Kylmälä, Finland*
[2] *Engineering Research Institute "Ventspils International Radio Astronomy Center", Ventspils University of Applied Sciences, Ventspils, Latvia*

Received 3 July, 2019

We present solar radio observations that were made semi-simultaneously with two Nordic–Baltic radio telescopes observing at two different frequency bands, 7.36 GHz and 37 GHz. The two radio telescopes are the Aalto University Metsähovi radio telescope located in Kylmälä, Finland, and the Ventspils International Radio-Astronomy Center (VIRAC) radio telescope located in Irbene, Latvia. The observations presented here were made between autumn 2017 and autumn 2018. We use them to study the active solar regions that are seen in the radio intensity maps at both frequencies. We find that the location of the maximum intensity is different for the two frequency bands, and that their peak intensities do not correlate. Based on these findings we propose a simplified scenario for how the radio sources can form at centimetre and millimetre wavelengths.

Keywords: Active region, sunspot, solar radio brightening, magnetic fields, radio telescope

1 Introduction

The connection between active regions and radio sources, such as their locational dependency, has been studied diversely over the past decades using solar radio maps, *e.g.* [Zhang et al. (2002), Gelfreikh & Shibasaki (1998)] and [Kallunki & Uunila (2017)]. Some scenarios have been presented for how the radio sources could form, recently *e.g.* [Smirnova et al. (2015)]. They propose that the rising magnetic fluxes from the active region form observable radio sources at centimetre and millimetre wavelengths. Additionally, it has been noticed that the locations of radio sources and optical active regions match so that the maximum intensity in radio intensity maps (I-maps) is near the position of the neutral line of the longitudinal photospheric magnetic field [Zhang et al. (2002), Smirnova et al. (2015)].

The earlier investigations have had one major limitation: they have studied the formation of radio sources using only one single radio frequency band (*e.g.* [Zhang et

*Email: juha.kallunki@aalto.fi

al. (2002)] and [Gelfreikh & Shibasaki (1998)]). In this research project we use two different radio frequencies, 7.36 GHz and 37 GHz. Hence, we can study the radio sources in two different solar atmospheric layers, from lower to upper chromosphere. It is also possible to estimate the spectral index of active regions by using two different radio frequencies. In Section 2 we present the instrumentation used in this study. The observations are shown in Section 3. And in Section 4 we propose a scenario for the formation of radio sources at centimetre and millimetre wavelengths. Also, we suggest some additional ideas for further development and research topics.

2 Instrumentation

The solar radio observations reported in this paper were made with the 32-m radio telescope (RT-32) of the Ventspils International Radio-Astronomy Center (VIRAC) at the wavelength 4.08 cm (7.36 GHz). This was the most sensitive band of the wide-band solar receiver, and the other bands were excluded from the analysis. The radio telescope is located in Irbene (E 21:51.17, N 57:33.12) about 35 km from the city of Ventspils. The location is rather optimal for radio astronomical observations due to low radio frequency interference (RFI) level. The bandwidth of this channel is 80–90 MHz and the beam size at this frequency is 5.34 arc min. The receiver is operated at room temperature, thus the noise temperature of receiver is approximately 290 K. The frequency 7.36 GHz is reported to correspond to solar brightness temperature 14605 K in the literature [Benz (2009)], but recent calibration observations gave a result of approximately 13300 K for the solar brightness temperature at 7.36 GHz [Bezrukovs et al. (2018)]. The measurements are always scaled relative to the Quiet Sun Level (QSL). The temporal resolution during observations is one second. It takes 30 minutes to make one solar radio map with RT-32. The full documentation of the RT-32 technical specifications can be found in [Bezrukov & Ryabov (2009), Bezrukov et al. (2017)].

The RT-14 at Aalto University Metsähovi Radio Observatory (MRO), Finland (Helsinki region; E 24:23.35, N 60:13.04) is a Cassegrain type antenna with a diameter of 13.7 m. The usable wavelength range of the telescope is 13.0 cm–2.0 mm. During solar observations the antenna is used for solar mapping, partial solar mapping, and tracking of any selected areas on the solar disk. The beam size of the telescope is 2.4 arc min at 8 mm. The receivers are Dicke-type radiometers. For the temperature stabilization of the two lower-frequency receivers, a Peltier element is used. The noise temperature of the 8 mm receiver is approximately 280 K. The temporal resolution during observations is 0.1 s or less. It takes approximately 180 seconds to make one solar radio map. The observational data are recorded in intensities. Because the measurements are always scaled relative to the QSL, the observations are comparable over the years. The brightness temperature of the QSL at 8 mm is 8100K $\pm$ 300K [Kallunki & Tornikoski (2018)]. The full documentation of the RT-14 technical specifications can be found in [Kallunki et al. (2012), Kallunki et al. (2018)].

The radio solar maps were also compared with magnetogram images from Magnetic Imager (HMI) on Solar Dynamic Observatory (SDO) satellite. HMI is one of three instruments aboard the SDO designed to study oscillations and the magnetic

field on the solar surface (photosphere level). HMI observes the full solar disk at 6173.3 Å with a resolution of 1 arc sec [Schou et al. (2012)].

3 Observations

Semi-simultaneous radio observations (solar radio intensity maps, I-maps) were made on four different days: 16 November 2017 (Figure 1), 21 December 2017 (Figure 2), 27 April 2018 (Figure 3), and 14 November 2018 (Figure 4). The strongest temperature contour is highlighted as a bold colour in Figures 1–4. The arrow in the middle of the contour represents the location of the maximum brightness temperature (intensity). On each day, there was an active region on the solar disk. A summary of the solar radio

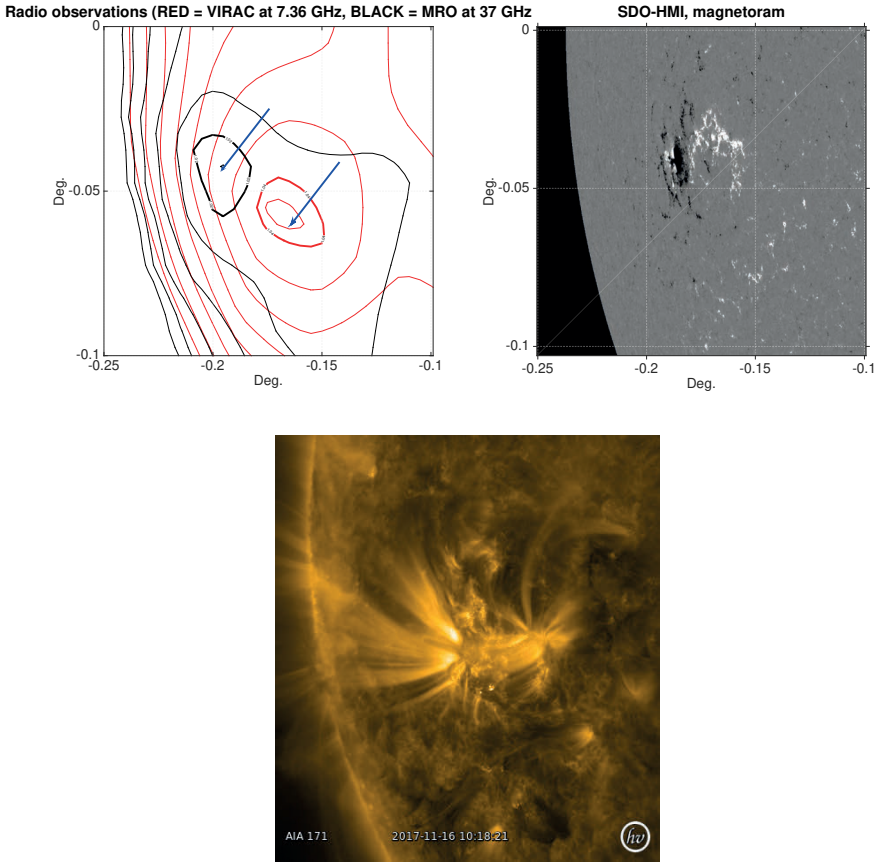


Figure 1 Observations made on 16 November 2017. In the upper left panel, we show an overlay of the two solar radio maps: the 7.36 GHz with red contour, the 37 GHz with black contour. In the upper right panel is the magnetogram observed with Helioseismic and Magnetic Imager (HMI)–Solar Dynamic Observatory (SDO) satellite. The locations of maximum radio intensities are marked with an arrow. In the lower panel, the active region at 171 Å is shown.

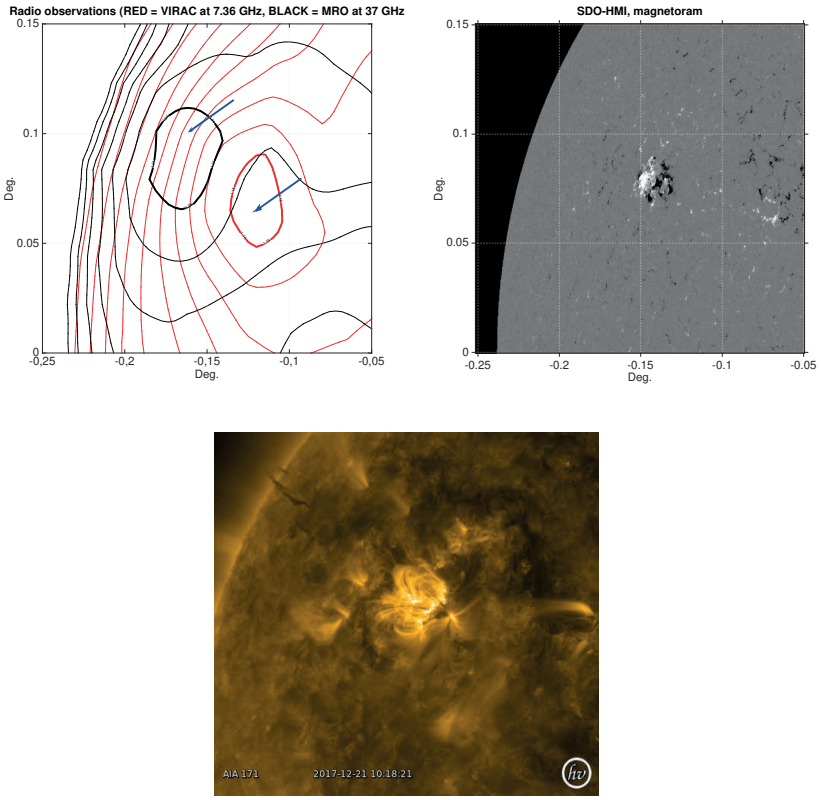


Figure 2 Observations made on 21 December 2017. The plots and symbols are as described in the caption of Fig. 1.

observations conducted in this project is presented in Table 1. All these active regions were non-flaring regions, thus no major flares or other activity were detected. The strength of the magnetic field (B) of the active regions was rather similar ($B \approx 720$–1300 G) in all four cases, and also the complexity of the active regions (Hale Class) was similar in all cases, see Table 1. The maximum intensity of these radio sources varied more, especially at 7.36 GHz (100.4 %–117.8 % relative to the QSL, 13349–15663 K). At the higher frequency, variations were smaller (102.6% –106.6 % relative to QSL, 8311–8643 K).

According to these observations, the maximum intensity is not at the same location at both frequency bands. Also, the maximum radio intensities (temperatures) between frequencies 7.36 GHz and 37 GHz do not correlate, as shown in Table 1. Furthermore, the locations of the maximum intensities on radio maps do not exactly match the location of the active region in optical data. We could not fully confirm that the maximum radio intensity is near the position of the neutral line of the longitudinal photospheric magnetic field of the magnetograms. Only in the first observation (16 November 2017), the radio intensity maximum at 37 GHz was close to the position of the neutral line. In the third observation (27 April 2018), the radio intensity at 7.36 GHz was close to the neutral line. In the fourth observation, the position of the

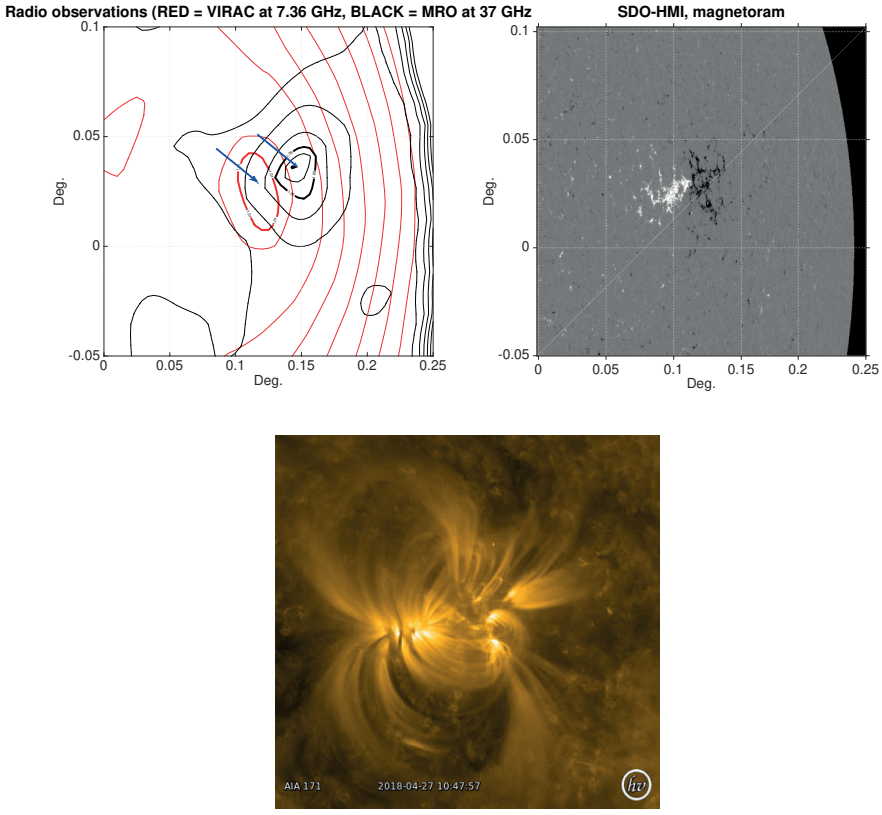


Figure 3 Observations made on 27 April 2018. The plots and symbols are as described in the caption of Fig. 1.

maximum radio intensity at 37 GHz is in the same location as the minimum magnetic field strength.

Table 1 Summary of observations: observing date, the maximum brightness temperatures relative to the QSL (in brackets the temperature difference from the QSL) and observing times (both MRO and VIRAC), magnetic field strength (both positive and negative polarities) and the Hale Class of the active region. For the last MRO observation (14.11.2018), the maximum brightness value could not be defined very reliably due to compromised weather conditions during the observing session.

Date	MRO, max. bright. (% to QSL)	MRO, obs. time UT	VIRAC, max. bright. (% to QSL)	VIRAC, obs. time UT	SDO HMI (+), G	SDO HMI (–), G	Hale
16.11.2017	102.6 (211 K)	10:22	105.3 (705 K)	10:29	1077	–956.4	β
21.12.2017	105 (405 K)	10:34	117.8 (2367 K)	10:19	1014	–1152	β
27.04.2018	106.7 (543 K)	09:59	101.6 (213 K)	10:49	1117	–1050	α
14.11.2018	103 (243 K)	09:44	100.4 (53 K)	10:49	1292	–723.7	α

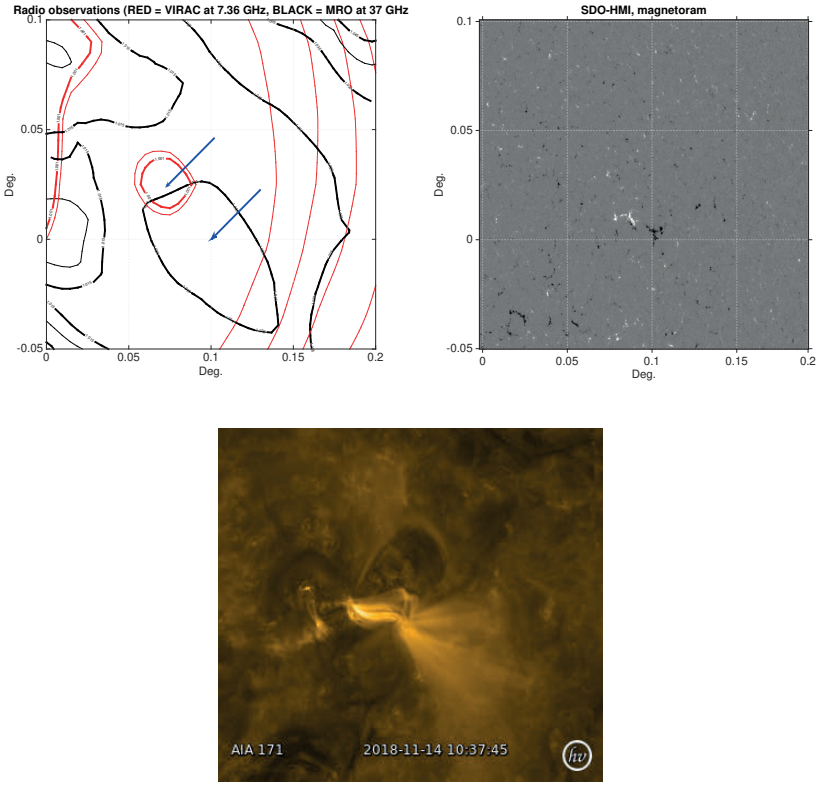


Figure 4 Observations made on 14 October 2018. The plots and symbols are as described in the caption of Fig. 1.

4 Results and conclusions

Sunspots or active regions form rising magnetic fluxes due to the thermalization of accelerated particles. These rising magnetic fluxes are observed as a radio source. Radio sources and visible sunspots or active regions are not observed exactly at the same locations. The magnetic fluxes do not rise fully vertically upwards. Smirnova et al. (2015) propose this scenario for forming radio sources at the millimetre wavelengths. However, the full scenario is most probably even more complex. There are several rising magnetic fluxes from the sunspot or the active region with varying heights, reaching the different solar atmospheric layers. Some of these rising fluxes reach the lower chromosphere (37 GHz emission) and some of them reach the higher chromosphere or transition region (7.36 GHz emission). Our observations support this interpretation, because the locations of maximum intensities are not the same at our observing frequencies (7.36 GHz and 37 GHz). The locations of the maximum intensities should be closer to each other if they originate from the same rising magnetic flux. In Figure 5, we present a possible scenario for forming radio source. Radio source 1 indicates the radio source observed at 37 GHz and Radio source 2 indicates

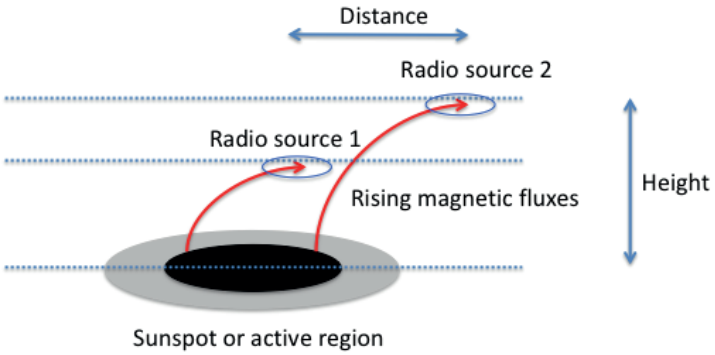


Figure 5 A proposed, simplified scenario for the formation of the observed radio sources. This model is an extension of the scenario presented by [Smirnova et al. (2015)]. The red arrows illustrate the rising magnetic fluxes. "Radio source 1" is observable at 37 GHz (lower chromosphere) and "Radio source 2" (upper chromosphere) is observable at 7.36 GHz. The lowest dashed line illustrates the photosphere level (optical active region or sunspot).

7.36 GHz emission source. This scenario is simplified, and radio sources can also form from several rising magnetic fluxes, not just one rising flux.

Furthermore, the maximum radio intensities of the two frequencies do not correlate. This result further confirms the interpretation that these radio sources are observed from different rising magnetic fluxes. There are varying strength rising magnetic fluxes.

The relatively low spatial resolution of radio observations might have some influence on the results. Also, the fact that all the four active regions were relatively close to the solar limb further complicates the analysis by possibly slightly distorting the projected view and the determination of exact locations.

When we compare the radio intensities between frequencies, we can see that in the first and the second cases (16 Oct 2017 and 21 Dec 2017) the spectral behaviour is similar and in the third case it is different, with larger temperature at as higher frequency. This could mean that the emission mechanism is different. Thermal bremsstrahlung could be the prevailing emission mechanism in the first and second events, while non-thermal gyrosynchrotron emission could be the prevailing emission mechanism in the third case [Dulk (1985)].

A larger number of simultaneous radio observations will be needed in order to confirm our findings. In addition, active regions of varying magnetic field strength should be included in the analysis. In this work, the observed active regions were almost of equal strength. It will also be important to observe active regions closer to the centre of the solar disk in order to exclude distortion effects from projection. It would also be interesting to analyse radio sources which are not identified with a sunspot or a visible-wavelength active region counterpart.

In this study we only used intensity maps (I-maps). It is possible to get circular polarization maps (V-maps) from the VIRAC radio telescope. These polarization features and properties should be studied in the future as well. Unfortunately, RT-14 only produces intensity solar radio maps on an irregular basis, but just recently, in spring 2019, the first polarization radio observations at 22 and 86 GHz have been

conducted with MRO-14. In addition, a more stable receiver at VIRAC, with a lower system noise, would make it feasible to include additional frequency bands in the multifreqeuency radio observing sessions. All these suggested improvements would help us better understand the solar atmospheric layers and solar radio physics.

Acknowledgements

The HMI data is courtesy of NASA/SDO and the AIA, EVE, and HMI science teams.

References

[Benz (2009)] Benz, A. O. 2009, Landolt Börnstein, 189

[Bezrukov & Ryabov (2009)] Bezrukov, D., Ryabov, B., 2009, Latvian Journal of Physics and Technical Sciences, vol.46, N.5, pp.46-58

[Bezrukov et al. (2017)] B. Ryabov, D. Bezrukov, J. Kallunki 2017, Latvian Journal of Physcis and Technical sciences 2017, vol.54, N. 3, pp.58-66

[Bezrukovs et al. (2018)] Bezrukovs, D., Kallunki, J., Ryabov, B. 2018, Space Research Review, Volume 5, 2018 pp. 16-28

[Dulk (1985)] Dulk, G. A., 1985, 23, 169

[Gelfreikh & Shibasaki (1998)] Gelfreikh, G. B., Shibasaki, K., 1998, CESRA Workshop on Coronal Explosive Events, 39

[Kallunki et al. (2012)] Kallunki, J., Lavonen, N., Järvelä, E., Uunila, M. 2012, Baltic Astronomy, 21, 255

[Kallunki & Uunila (2017)] Kallunki, J., Uunila, M. 2017, Astronomische Nachrichten, 338, 398

[Kallunki & Tornikoski (2018)] Kallunki, J., Tornikoski, M. 2018, Sol. Phys, 293, 156

[Kallunki et al. (2018)] Kallunki, J., Tornikoski, M., Tammi, J., et al., 2018, Astronomische Nachrichten, 339, 204

[Schou et al. (2012)] Schou, J., Scherrer, P. H., Bush, R. I., et al., 2012, Sol. Phys., 275, 229

[Smirnova et al. (2015)] Smirnova, V. V., Solov'ev, A. A., Riehokainen, A., Kallunki, J. 2015, Geomagnetism and Aeronomy, 55, 991

[Zhang et al. (2002)] Zhang, C.-X., Gelfreikh, G. B., Wang, J.-X. 2002, Chinese J. Astron. Astrophys., 2, 266